University of Thi-Qar Journal of Science (UTJsci)
E-ISSN:2709-0256, ISSN Print: 1991-8690 Volume (10), No.1, June 2023

Nonlinear Quantum Dot Light Emitting Diode Dynamics and Synchronization with Optoelectronic Feedback

Methag Abdalwahed Kadim
Thi Qar education directorate
Thi Qar/ Iraq
methag6999@gmail.com

Sadiq Kh. Ajeel
Dept. of Physics/College of Science,
University of Thi Qar
Thi Qar/ Iraq
sadeq.ajeel@sci.utq.edu.iq

Ali Natheer Tuaimah
Dept. of Physics/College of Science,
University of Thi Qar
Thi Qar/ Iraq
alinatheer_ph@sci.utq.edu.iq

Ali Falah Hassan
Thi Qar/ Iraq
Aliflah1988a@gmail.com

Sora F. Abdalah
Istituto Nazionale di Ottica- CNR,
Largo E. Fermi 6, 50125
Firenze, Italy
sora.abdalah@ino.it

Kais A. Al Naime
Dept. of Physics/College of Science,
University of Baghdad
Baghdad/ Iraq
kais.al-naimee@ino.it

Riccardo Meucci
Istituto Nazionale di Ottica- CNR,
Largo E. Fermi 6, 50125
Firenze, Italy
riccardo.meucci@ino.it

Amin H. Al Khursan
Dept. of Physics/ College of Science,
University of Thi Qar
Thi Qar/ Iraq
ameen_2all@yahoo.com

Ali. H. Khidhir
Dept. of Physics/College of Science,
University of Baghdad
Baghdad/ Iraq
alzurfialiali@gmail.com

Hussein B. Al Husseini
Dept. of Physics/ College of Science,
University of Thi Qar
Thi Qar/ Iraq
drhussain@sci.utq.edu.iq

***Abstract*— As a three-variable dimensionless model, we look into the optoelectronic feedback (OEFB) of a quantum dot light emitting diode (QD-LED). We examine complex bifurcation scenarios for photon intensity together with time series, fast Fourier transform (FFT), and attractor of all dynamic variables in order to better understand the dynamics of the QD-LED. The bifurcation graphic shows that the chaotic dynamics of the QD-LED is completely controlled by the OEFB strength and delay-time fluctuations. Our results show that the light transmitted to the OEFB recurs regularly under a short delay time. Additionally, we investigate the synchronization of chaos in two QD-LEDs that are coupled via a unidirectional and bidirectional coupling scheme. When periodic systems are non-identical, both unidirectional and bidirectional systems depending on the coupling strength parameter the system exhibits complete synchronization. Residual chaos, the mean coherence and entropy are discussed as well.**

***Keywords*— QD-LED, OEFB, chaos synchronization, residual chaos, entropy.**

I. INTRODUCTION

Within the past years control of complex dynamics has evolved as one of the central issues in applied nonlinear science [1]. Moreover, time-delayed feedback loops might be deliberately implemented to control neural disturbances, e.g., to suppress undesired synchrony of firing neurons [2-4].

Quantum dots (QDs) are grown by the self-assembling process into a wetting layer (WL), two-dimensional quantum-well layer. Thus, QD structure consists of completely quantized subbands in the QDs attached with the two-dimensional WL. QD light emitting diodes gets attention recently due to their superior characteristics and wide range of applications [5, 6].

The QD-LED can be perturbed using an OEFB circuit. A key function in the QD dynamics is shown by the phase sensitivity of optical feedback in QD lasers [7]. Contrary to optical feedback, however, we do not need to take the phase effect into account in an OEFB circuit because the phase information is already eliminated by a photo-detector during the feedback process [8]. Through the injection current, optical device functions that are stable or unstable are

https://doi.org/10.32792/utq/utjsci/v10i1.1055

reliably and compliantly managed [9, 10]. There are two groups for OEFB: one is for negative feedback, the other is for positive feedback. They each use a unique set of driving mechanisms to control the dynamics of the light output. In the first type (negative feedback), the current of feedback is subtracted from the current of bias injection, which causes the relaxation oscillation to become sharper [11]. On the other hand, semiconductor lasers have both positive and negative self-sustained pulsations. Their dynamics, however, are not always the same. For instance, whereas they are infrequently found in positive OEFB, the states of the frequency locking are characteristic of negative OEFB [12]. Synchronization of two chaotic systems can be achieved using different coupling schemes under unidirectional [13, 14] or bidirectional configuration [15, 16] which can be either optical or optoelectronic, direct or delayed [17, 18]. The majority of scientific investigation on the methods and properties of chaotic synchronization were concentrated on the unidirectional coupling between the oscillators in a transmitter (T) – receiver (R) configuration where the dynamics of the T system are reproduced by the R system.

In the following, we first give here a rate equation analysis that takes into account the crucial elements of electronic transitions. In order to explain the extraordinarily complex behavior and modulation rate of QD-LEDs, we apply the examination to a rate equations model of the states of the three levels in dimensionless form. This model takes into account both photon reabsorption and non-radiative recombination processes. And secondly, we discuss the OEFB properties when small and large delay time and feedback strength is applied to QD-LED. Then, we study coupled two chaotic systems subject to time delayed OEFB under unidirectional and bidirectional chaos synchronization, as a result, although synchronization in QD-LED is difficult to attain, it is obtained at some points corresponding to some periodic states.

As the long delay duration and the negative feedback strength are changed in this study, we negotiate a rich bifurcation demonstration. Chaotic behaviors are distributed in tiny delay time value areas together with periodic and quasi-periodic ones and multi-stability of various types of attractors, which is a common characteristic. We discover that the quasi-periodic state is the pathway by which the OEFB of QD-LED arrive chaotic. This is in good agreement with the findings of analytical bifurcation analysis of the system modeled as delay differential equations [19].

II. QD-LED MODEL WITH OEFB

In the rate equations system, a term is added to the pumping to represent the OEFB effect. In the QD-LED system, the electrons are first pumped into WL before being collected by the QDs. The dynamics of the number of carriers in the QD ground state n_{QD} , n_{wl} which is the number of carriers in the WL, and the number of photons in the optical mode S are described by the rate equations shown below:

$$S^{g} = A\, n_{QD} - \alpha S - \gamma_s S \quad ,$$

$$n_{QD}^{g} = \gamma_c n_{wl}\left(1-\frac{n_{QD}}{2N_d}\right) - \gamma_{r_{QD}} n_{QD} - \left(A n_{QD} - \alpha S\right)$$

$$n_{wl}^{g} = \frac{I}{e}\left(1+\frac{k\,S(t-\tau_s)}{S_o}\right) - \gamma_{r_{wl}} n_{wl} - \gamma_c n_{wl}\left(1-\frac{n_{QD}}{2N_d}\right) \qquad (1)$$

In our system, the photon number, $S(t-\tau_s)$, is fed from the external OEFB circuit to the QD-LED which is added to pumping in the third equation of the system. Where k is the strength of the feedback. For a positive value of k , the system is in positive feedback, while for a negative value it is in negative feedback. S_o is the photon number at the steady state value. τ_s is the delay time taken by the feedback signal. Here, A is called the spontaneous emission rate into the optical mode, $\gamma_{r_{QD}}$ and $\gamma_{r_{wl}}$ are the rates of non-radiative decay of the number of carriers in the WL and QD respectively; N_d is the total number of QDs; and e is elementary charge, I is the injection current, , α and γ_s are the absorption and output coupling rate of photons in the optical mode, respectively, γ_c is the capture rate from WL into the dot.

For a three-level microscopic system where the transition is homogeneously broadened, it can be shown from the Einstein relation that [20]

$$\alpha = A\Gamma n_o \qquad (2)$$

Where the optical confinement factor is Γ and the initial carrier occupation number of the QDs is n_o . The spontaneous emission coefficient and the absorption coefficient have similar line forms in this situation. Both the QD and WL states can be in homogeneously widened for actual QD material systems. In order to establish the proper relationship between absorption and spontaneous emission spectra, population distributions in both QD and WL are explicitly taken into consideration. A QD-LED's OEFB is schematically depicted in Fig. 1.

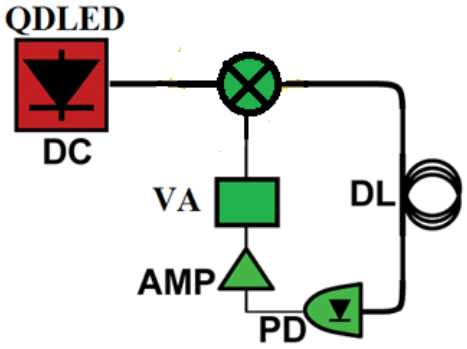

Fig. 1. Shows the OEFB structure schematically; the nonlinearity caused by the maxing is external to the output. Quantum dot light emitting diode, photodiode, amplifier, variable attenuator, and optical delay line are all abbreviations for the same device .

We rescale the rate equations to typical equations without dimensions after applying the OEFB term to the QDL-EDs equation system. Important new parameters with no dimensions are considered as follows

$$x = S, \quad y = \frac{A}{\gamma_s}(n_{QD} - \Gamma n_o S),$$

$$w = \frac{n_{wl}\gamma_c}{A}, \quad \gamma_{r_{wl}} = \frac{t'}{t}, \tau = \frac{\tau_s}{\gamma_{r_{wl}}}$$

$$\gamma = \frac{\gamma_s}{\gamma_{r_{wl}}}, \quad \gamma_1 = \frac{A}{\gamma_{r_{wl}}}, \ \gamma_2 = \frac{A}{\gamma_s}, \ \gamma_3 = \frac{\gamma_{r_{QD}}}{\gamma_{r_{wl}}}, \ \gamma_4 = \frac{\gamma_c}{\gamma_{r_{wl}}},$$

$$N_d \equiv a, \ \Gamma n_o \equiv b \ and \ \delta_o = \frac{I}{Ae} \ .$$

The system in equation (1) can be rewritten in the following form,

$$x^{g} = \gamma\left(y - x\right),$$

$$y^{g} = \gamma_1\gamma_2 w\left(1 - \frac{b}{a}x\right) - \gamma_1 y\left(1 + \frac{1}{a}w\right) - b\gamma_1\left(x - y\right)$$

$$-\gamma_3\left(y + b\gamma_2 x\right),$$

$$w^{g} = \gamma_4\delta_o\left(1 + \frac{k\,x_\tau}{x_o}\right) - w\left(1 - \frac{\gamma_4}{a\gamma_2}y\right) - \gamma_4 w\left(1 - \frac{b}{a}x\right) \qquad (3)$$

Here, the upper subscript "dot" (g) refers to differentiation with respect to (t'). The bias current is represented by (δ_o).

III. Results of QD-LED with OEFB

First, we discuss chaotic evolution of pulsing states in negative OEFB systems. The rate equations system with Eqs. (3) is solved numerically using the fourth-order Runge-Kutta method by Matlab programming. The used parameters in the simulation are listed in Table 1. Solving the system (3) at a steady state yields the initial values.

Table 1. Unless otherwise noted, numerical parameters were employed in the simulation [23].

Parameters	value	Parameters	value
x_{oT}	0.066	γ_2	0.03
y_{oT}	0.99	γ_3	0.07
w_{oT}	0.0049	γ_4	0.087
γ	0.172	a	1.04
γ_1	0.144	b	3.838
x_{oT}	0.022	τ_T	2800
y_{oT}	1	τ_R	1800
w_{oT}	0.01	τ_C	2800
k_T	± 0.05	k_R	± 0.002

The time series of the QD-LED's light output (photons number) is depicted in Fig. 2. The middle and left pillars, respectively, display the agreeing attractors at various time delays and the Fourier transform of the output spectrum that corresponds to them, known as the fast Fourier transform (FFT). The rummage-sale settings are feedback strength k=0.2 for QD-LED and current of bias δ_o=1.6. The theoretical time series is used to reach the attractor in a space where delays are embedded. Fig. 2 (a)–(c) was captured at delay times of τ = 40, 42, and 44, respectively.

The time series can clearly be seen transitioning from periodic oscillations that occur on a regular basis Fig. 2(a) to quasi-periodic oscillations with intensity amplitudes adjusted at a certain doubling frequency Fig. 2(b). Last but not least, the dynamics eventually enter a chaotic stage in which the intensities fluctuate erratically Fig. 2(c). A good agreement between the chaotic state and the experimental and numerical results for LED as a bulk is shown in Fig. 2(c). The FFT shows that there are only a small number of fundamental frequencies, as seen in Fig. 2(a). The little spectra ripples suggest a slight degree of QD-LED instability. More frequencies that correlate to a quasi-periodic oscillating condition are shown in Fig. 2(b).

Finally, as the system transitions toward a chaotic state in Fig. 2(c), the spectrum broadens and dense, sharp spectral peaks arise. The large cycle in Fig. 2(a) corresponds to regular periodic oscillations for the attractor column. The cycle's size provides a clue as to whether the data are periodic. Despite the quasi-periodic case, each one has a diffused closed curve and has a toroidal attractor characteristic as seen in Fig. 2(b). The spread of the attractor plot in Fig. 2(c) illustrates a change from order to chaos.

When the delay durations are τ = 14.2, 24.2, 34.2, and 40.2, Fig. 3 displays a repeated periodicity at the same parameter values for the bias current (δ_o =1.6) and feedback intensity (k=0.2). Their attractor also shown that this periodicity does not reoccur after = 40.2. Be aware that between these delay times, different dynamics, ranging from periodic to chaotic, are obtained. This recurring periodicity may be explained by the brief delay time (τ), which does not significantly disturb the system. As a result, after a certain wait, it resumes its periodic state.

In the case of negative feedback Fig. 4(a), the system first displayed chaotic pulsing up to a value of τ = 800, after which it entered two states: one characterized by chaotic and periodic pulsing, and the other by a periodic state at $\tau \geq 1000$. For positive feedback, the system in Fig. 4 (b) started chaotically pulsating until τ = 850, at which point it used the chaos to induce a regular state until it reached a regular state for $\tau \geq 1000$. Fast inter-dot dynamics are related to examples of high dynamics for short delays in QD lasers with OEFB circuits [22].

Chaotic states are rich for negative case. Fig.5 presents the bifurcation diagram of feedback strength. Different bias are used for negative (δ_o = 5.6) and positive (δ_o = 0.6) cases. A dense chaos is obtained compared with Fig. 4. Note that the positive case is an inverted replica of negative one. We note that the negative feedback is richer in terms of dynamics than the other type.

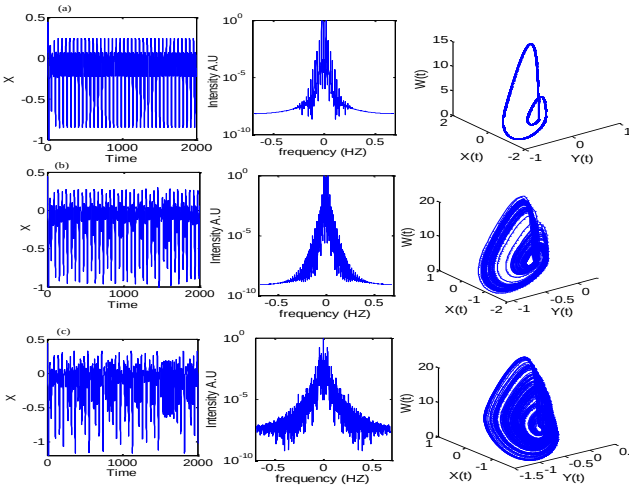

Fig. 2. Numerical results: (left column) time series, (mid column) FFT and (right column) attractor sections at different values of the delay times. From top to bottom: (a) periodic oscillations, at τ =40; (b) two-frequency quasi-periodicity, at τ = 42; (c) chaos, at τ =44. The broadband related in (c) is much higher than in (b). The parameters stately are δ_o=1.6 and k=0.2.

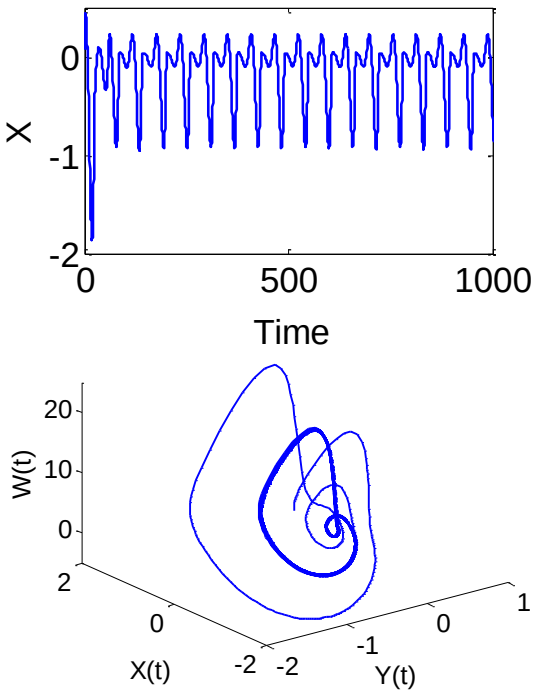

Fig. 3. Time series, and attractor in three dimension of different pulsing states: regular periodic pulsing at τ=14.2. In the theoretical simulations, the parameters are expected to be δ_o=1.6 and k=0.2.

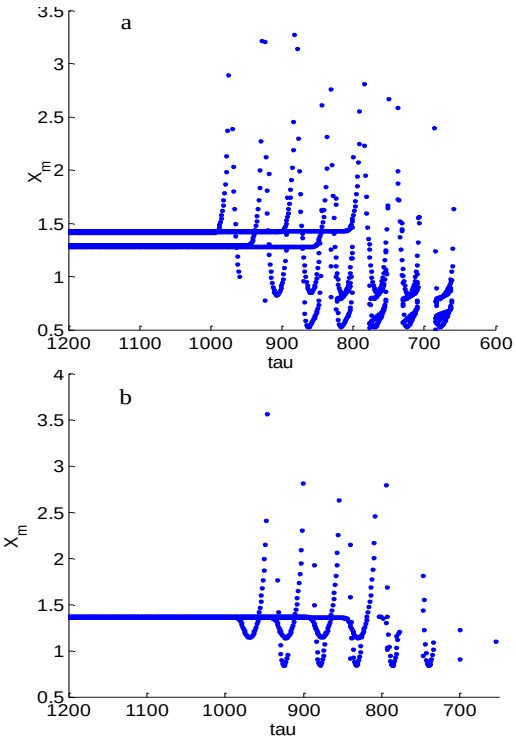

Fig.. 4. Positive feedback strength (b) and negative feedback strength (a) of the peak series of the photon density extrema, with normalized delay time (NDT) increasing inversely from 1200 to 600. The parameters for the numerical simulations are taken to be δ_o =5.6 and k=0.2.

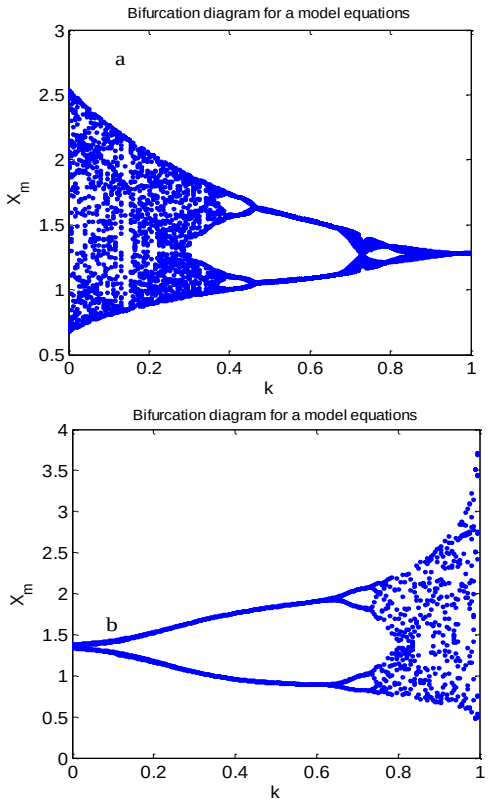

Fig. 5. Bifurcation diagrams of the photon density (a) negative feedback strength and (*b*) positive feedback mode in dependence of the feedback strength *K* for small value of δ_o=0.6 (a) and another large δ_o=5.6 (b) and delay time τ =1500.

IV. UNIDIRECTIONAL SYNCHRONIZATION IN QD-LED

We discussed chaotic oscillations in OEFB in QD-LED in section III. In this section the chaotic synchronization of coupling unidirectional system with OEFB was studied. In OEFB systems, the rate equations for the photon and carrier number are enough for describing the systems. OEFB systems in laser have an advantage of excellent synchronization over other optical feedback systems. Since the time scale of carrier is three orders larger than that of the photon lifetime [8]. Synchronization is studied briefly in bulk LED [21]. There are no work deals with it in QD-LED. The rate equations for the photon and carrier number in QD and WL in a T and R of OEFB are written by

$$x^{g}_{T,R} = \gamma\left(y_{T,R} - x_{T,R}\right)$$

$$y^{g}_{T,R} = \gamma_1\gamma_2 w_{T,R}\left(1-\frac{bx_{T,R}}{a}\right) - \gamma_1 y_{T,R}\left(1+\frac{w_{T,R}}{a}\right) - b\gamma_1\left(x_{T,R} - y_{T,R}\right) - \gamma_3\left(y_T + b\gamma_2 x_{T,R}\right),$$

$$w^{g}_{T,R} = \gamma_4\delta_o\left(1+k_{T,R}\, x_{\tau_{T,R}} + \delta k_c\, x_{\tau_T}\right) - w_{T,R} \times\left(1-\frac{\gamma_4 y_{T,R}}{a\gamma_2}\right) - \gamma_4 w_{T,R}\left(1-\frac{bx_{T,R}}{a}\right) \qquad (4)$$

Where $k_{T,R}$ is the coefficient of the OEFB strength in the T and R. δ = 0 in T rate equations and δ = 1 in R rate equations. The schematic setup of the synchronization is shown in Fig. 6 (a).

As in our model on the synchronization of QD-LED, we include the factor k_c, with $0 \le k_c \le 1$, to indicate the percentage of the total coupling signal strength in the R from the R. When k_c =0 there is no coupling in the R and it is called open loop. When k_c =1 the T and R are completely coupled. We denote the transmission time by τ_c; the time associated with the propagation of the signal to the R system. A state of complete synchronization is attained in case of identical T and R systems, where the dynamical variables of both are equal. Thus, the case of identical systems was not discussed in this work.

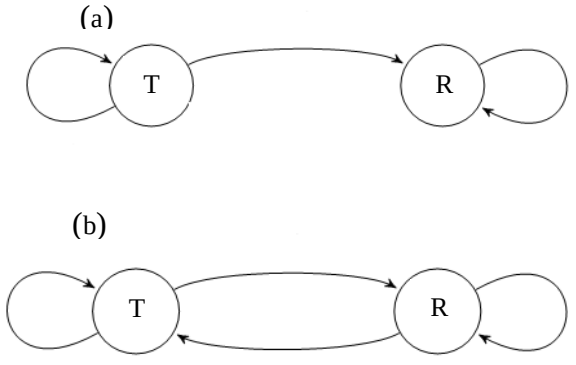

Fig. 6. Schematic for the synchronization of two chaotic systems with delayed OEFB of QD-LED. (a) unidirectional synchronization, (b) bidirectional synchronization [24],

V. RESULTS OF UNIDIRECTIONAL SYSTEM

Fig. 7 shows a comparison between the output of x_T and x_R before, Fig. 7 (a) (τ_c =0 and k_c=0) and after, Fig. 7 (b), (τ_c =1800 and k_c=0.45) coupling, respectively, at τ_t = τ_r = 1800, k_t=0.69, k_r=0.06 and δ_o=0.6. Their corresponding correlation plots are shown in Fig. 7 (c) and (d), respectively. Fig. 7 (c) shows uncorrelated behavior between T and R, only a few symmetries were shown due to the same bias current used which results in the same height of photon output of T and R. For the correlation plots, Fig. 7 (d) shows a better correlation obtained between these two chaotic systems when they are coupled. To explain these plots, their attractors are shown in Fig. 8 for QD (Fig. 8 (a) and (b)) and for WL (Fig. 8 (c) and (d)). It was shown that the chaotic behavior comes from WL, this corresponds that it is a highly condensed state (continuums state) and long relaxation time compared with QD.

VI. RESIDUAL CHAOS , MEAN COHERENCE AND ENTROPY

The residue of chaos synchronization can be defined by the following equation[25]:

$$R_{chaos} = \left|\frac{x_{T_{\max}} - x_{R_{\max}}}{x_{T_{\max}}}\right| \qquad (5)$$

Where x_T and x_R are the maximum intensities of the T and R QD-LED systems. To imply more detailed discussion for synchronization, a different feedback cases are imposed with negative and positive feedback strengths for each of the two systems. Note that residual chaos attractor was introduced here for the first time.

To describe qualitatively sudden transition between synchronization and non-synchronous cases, we characterized the degree of ordering in the system by means of the entropy (S). By extracting the S value in synchronization and non-synchronization states. S is calculated from the distribution of the response times t_r in the time series using the relation [23]:

$$S_i = \sum_j\left[x_i(t_r)\ln\frac{x_j(t_r)}{x_i(t_r)}\right] \qquad (6)$$

VII. RESULTS OF RESIDUAL CHAOS, MEAN COHERENCE AND ENTROPY

Several numerical results appear in Fig. 9 for the systems parameter values τ_t= τ_c= 2800, τ_r= 1800, k_t= 0.05, k_r = 0.002 and δ_o = 2.7 used as a control parameter to select different dynamical behaviors. Fig. 9 shows residual chaos plots (left panel) and entropy (right panel). In Fig. 9 (a) for negative feedback strength of T and R, a stable solution is obtained when k_c = -0.4 where synchronization of the photon and carrier numbers in T and R is accomplished. For positive OEFB for both T and R, Fig. 9 (b) shows that the synchronization is obtained only when k_c = 0.1. In Fig. 9 (c) the residual of positive T and negative R have no synchronization. Fig. 9 (d) shows the residual for negative T and positive R, the synchronization is obtained k_c = -1 with positive curve inclination.

Fig. 9 (right panel) shows distribution (S) location which is shifted according to synchronization points shown

in the left panel. We also find that the T output is still fixed while the R output is shifting since the T is demonstrated.

To explain residual, time series and their correlations of two points from Fig. 9 (a) are plotted. Taking k_c = 1 as a highest residue, their plots are shown in Fig. 10 (a) and (b) while Fig. 10 (c) and (d) shows the plots of the case k_c = -0.4 as the synchronization point. While some symmetry can be detected at some directions in Fig. 10 (b) compared with Fig. 8 (c), a lag was obtained in Fig. 10 (d) which refers to high symmetry between T and R, this latter case corresponds to their periodic states. This is enough to explain all other residue points.

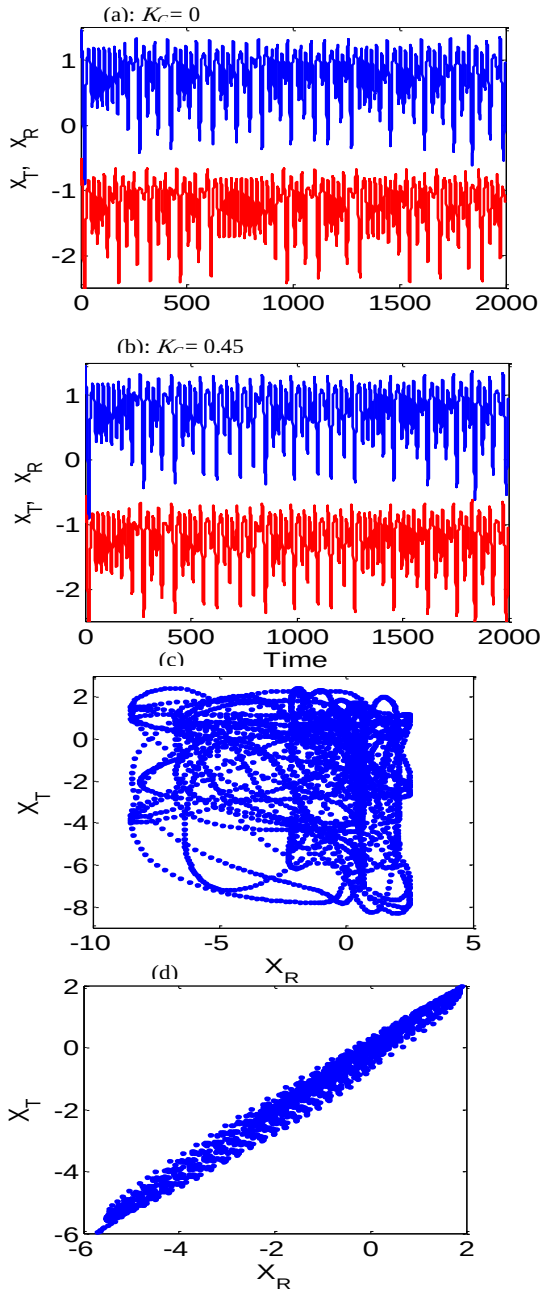

Fig. 7. Comparison of the chaotic waveforms and the correlation plots under the condition k_c =0 as in (a). (a) Chaotic waveforms from the outputs of the T (upper trace) and the R (lower trace). And under the condition k_c =0.45 as in (b). (b) Chaotic waveforms of the driving signal (upper trace) and the output of the R (lower trace). (c) Correlation plot between the two traces in (a). (d) Correlation plot between the two traces in (b). The T and R under unidirectional coupling with delayed time τ_t=τ_r=τ_c=1800. Others parameters are used k_t=0.69, k_r=0.06 and δ_o=0.6

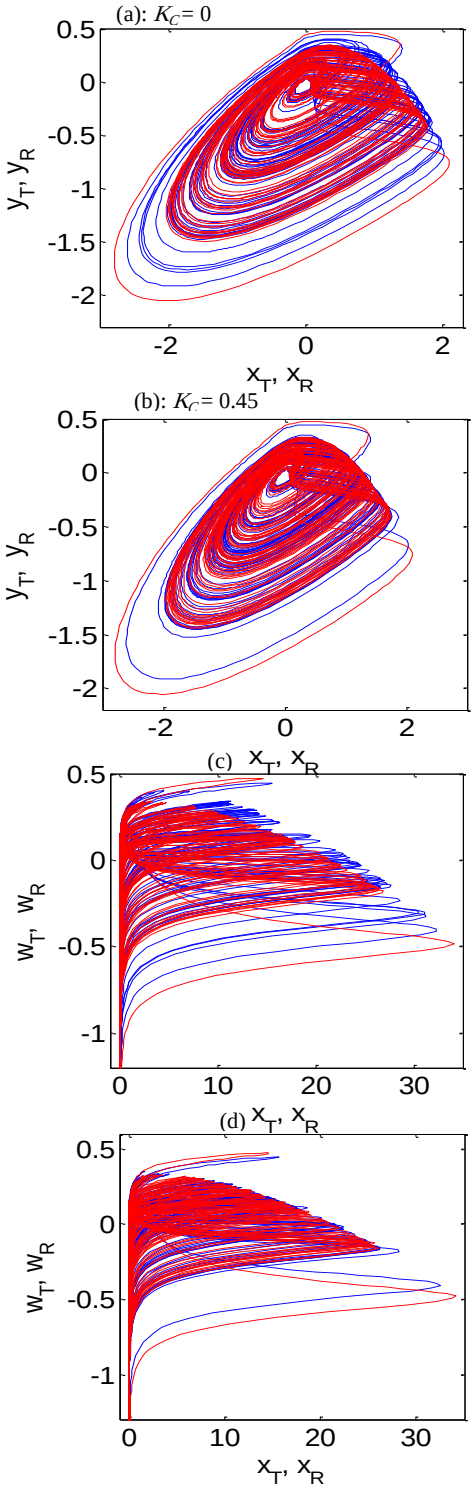

Fig. 8. Chaotic attractors in the phase space of QD-LED output (T and R, respectively), QD carrier y, and WL carrier w. (a) and (b) attractors correspond to Fig. 7. (a) and (b). (c) and (d) attractors correspond to Fig. 7. (c) and (d).

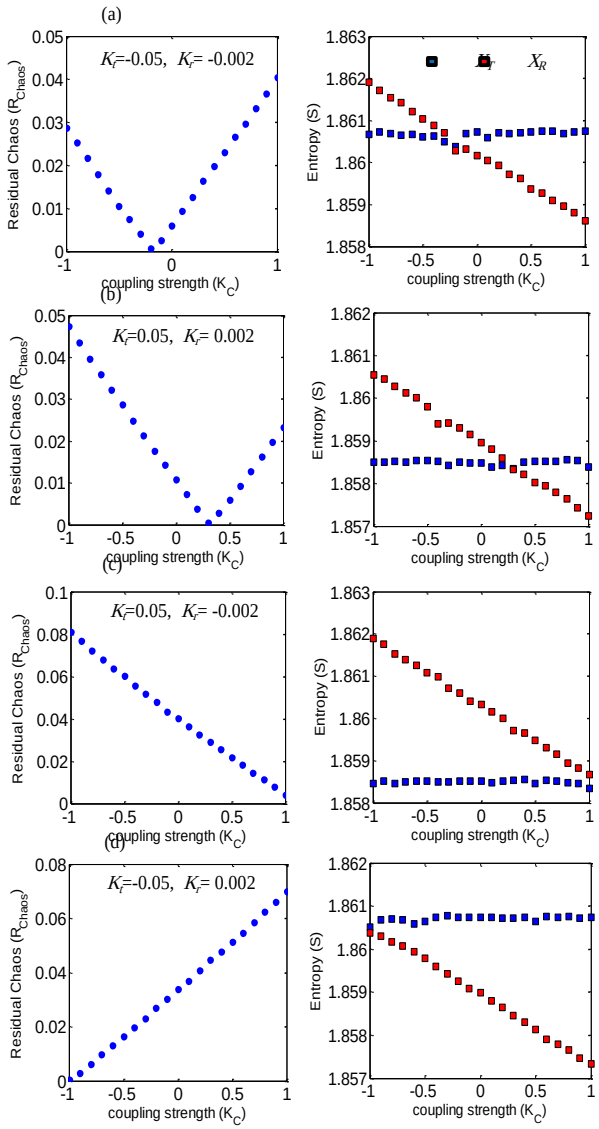

Fig. 9. Calculated residual chaos and the entropy of two chaotic systems as a function of coupling strength. The chaotic systems unidirectional synchronization is done with four different cases of feedback signal strength in the R and T. The parameters are used in Table 1

VIII. Bidirectional Synchronization in QD-LED

Its advantage is that one needs to calculate the other kind of coupling between two chaotic systems explicitly for the particular synchronized dynamics. In contrast, to unidirectional, in bidirectional coupling is necessary and sufficient to study the exerted synchronization due to the effect of two chaotic systems on each other; however, its strength depends solely on the coupling topology, i.e. the eigenvalues of k_c and not only on the particular dynamics of the system, the case of unidirectional.

Consider two chaotic systems that are coupled to each other with a coupling delay and additional self-feedback of R and T with the same delay time τ. The basic coupling scheme is depicted in Fig. 6 (b). The coupled system is described by dimensionless rate equations type.

$$w^{g}_{T,R} = \gamma_4 \delta_o (1 + k_{T,R}\, x_{\tau_{T,R}} + k_c\, x_{\tau_{T,R}}) - w_{T,R} \times \left(1 - \frac{\gamma_4 y_{T,R}}{a\gamma_2}\right) - \gamma_4 w_{T,R}\left(1 - \frac{b x_{T,R}}{a}\right) \qquad (7)$$

The same system parameters used in unidirectional case are used here which are listed in Table 1.

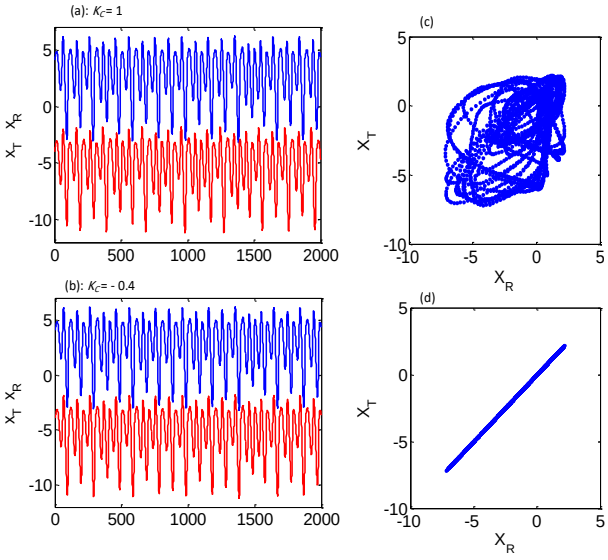

Figure. 10 Comparison of the output and the correlation lag plots under the condition k_c =1 as in (a), the outputs of the T (upper trace) and the R (lower trace). And under the condition k_c = -0.4 as in (b), the driving signal (upper trace) and the output of the R (lower trace). (c) Correlation lag plot between the two traces in (a). (d) Correlation plot lag between the two traces in (b). The T and R under unidirectional coupling with delayed time τ_t= τ_c= 2800 and τ_r=1800. Others parameters are used k_t=-0.05, k_r=-0.002 and δ_o=2.7.

IX. Results of Bidirectional System

It is well known that chaos synchronization is possible if the self-coupling of the R system is weaker than that of the T system [24, 26]. Fig. 11 (a)-(d) (left) shows residual chaos of bidirectional system. From these figures, bidirectional synchronization in QD-LED with OEFB circuit exhibits some features: at all cases coupling strength, $|k_c|$, is smaller than 0.5; the coupling strength has a different polarity for similar polarity of T and R as in Fig. 11 (a) for positive T and R and Fig. 11 (b) for their negative while the receiver polarity was controlling in case of different T and R polarity as in Fig. 11 (c) and (d). Note that this behavior can be explained as a result of the shared polarity of both T and R systems which is in the contrary of unidirectional synchronization where only polarity of the T system was dominant.

The entropy of the bidirectional system was shown in the right panel of Fig. 11 (a)-(d). While the T system is constant in unidirectional case as in Fig. 8, in bidirectional case both the T and R are correlated and changed with coupling strength. Fig.12. Calculated residual chaos and the mean coherence value (row one). Entropy chaos synchronization for amplitude and the entropy for phase synchronization (row two), green and yellow squares represent the T and R

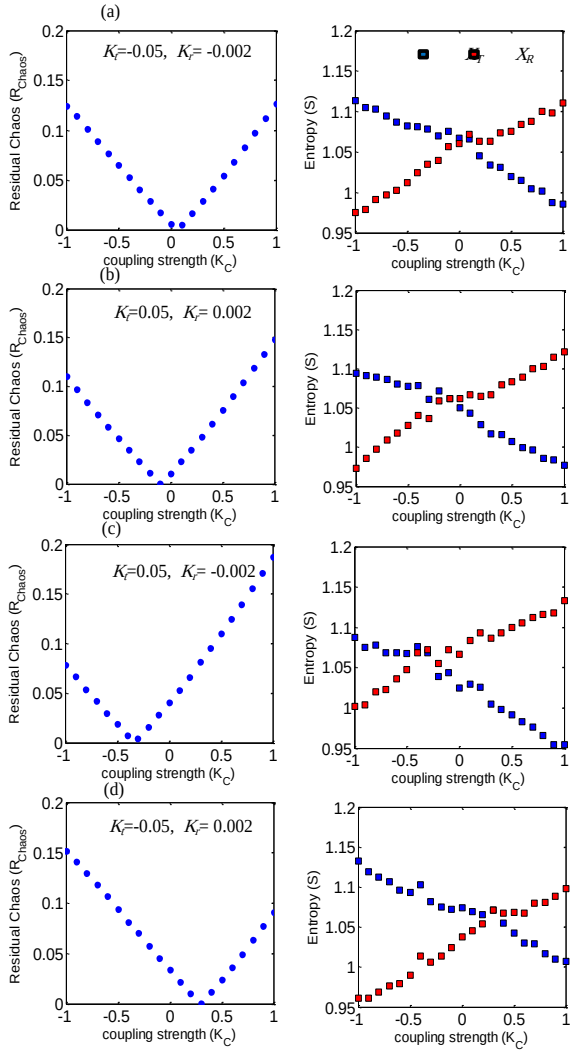

Fig. 11. Calculated residual chaos and the entropy of two chaotic systems as a function of coupling strength. The chaotic systems bidirectional synchronization is done with four different cases of feedback signal strength in the R and T. The parameters are used in Table 1.

signal respectively. The correlation coefficient between the absolute mean value of outputs of the T and the R. The two chaotic systems as a function of coupling strength. Quality of chaos synchronization under different coupling strengths. The chaotic systems unidirectional synchronization is done with ξ_r=0, ξ_t= -0.05. The parameters are used in Table 1 and recent our work [27-28].

X. Conclusion

In this study, we demonstrate the existence of complicated physical dynamics in a connected OEFB QD-LED. The system rate equations model is changed to a dimensionless form, and the results show that chaotic states can emerge from periodic states when delay times and deception feedback strengths are changed. Protective delay-time and changing feedback strength provide the rich chaotic. However, it is important to highlight that findings are shown in cases when the feedback strength is variable and the dynamical behavior is incongruent. The chaotic behavior could be calculated in terms of FFT and attractor corresponding to time series, where chaotic happened at τ = 44 as small delay and least than τ= 950 as large delay in bifurcation diagram. Besides, we have discussed chaos synchronization conditions for optoelectronic coupled QD-LEDs. A different kind of controlling the synchronization phenomenon as reported. This approach allows controlling the parameter mismatch between the coupled units, what usually occurs in the theoretical methods. Here, the interaction of the optoelectronic units has been reached through adjustment of the system states whereas the phase effect is neglected. Moreover, we have realized theoretical synchronization in terms of the chaos synchronization residue, entropy and lag of the response times, measured between interacting QDLEDs units. From both the chaos synchronization unidirectional and bidirectional have been evaluated what revealed the positive and negative effect in its value as the coupling strength was modulated.

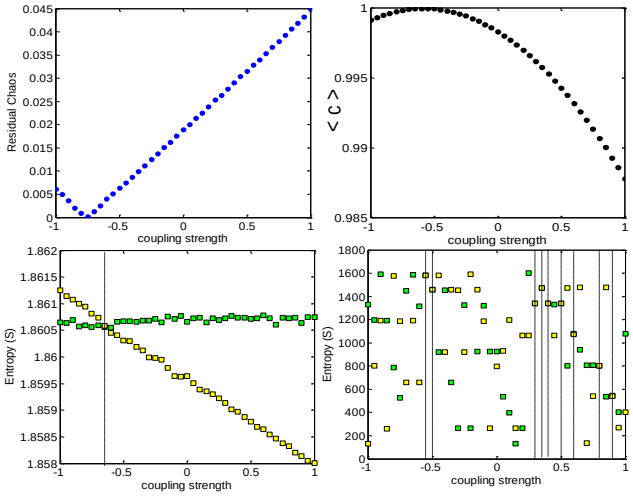

Fig. 12. Calculated residual chaos and the mean coherence value (row one). Entropy chaos synchronization for amplitude and the entropy for phase synchronization (row two), green and yellow squares represent the T and R signal respectively. Correlation coefficient between the absolute mean value of outputs of the T and the R. The two chaotic systems as a function of coupling strength. Quality of chaos synchronization under different coupling strengths. The chaotic systems unidirectional synchronization is done with ξ_r=0, ξ_t= -0.05. The parameters are used in Table 1.

Conflict of Interest

Authors declare that they have no conflict of interest.

References

[1] E. Scholl and H. Schuster: Handbook of Chaos Control, Wiley-VCH, Weinheim, 2008.

[2] H. Haken, Brain Dynamics: Synchronization and Activity Patterns in Pulse-Coupled Neural Nets with Delays and Noise, . Springer Verlag GmbH. Berlin. 2006.

[3] B. Hauschildt N. B. Janson, A. G. Balanov and E. Scholl, Noise-induced cooperative dynamics and its control in coupled neuron models. Phys. Rev. E 74, 051906. 2006.

[4] P. Hovel, M. A. Dahlem and E. Scholl, Control of synchronization in coupled neural systems by time-delayed feedback. Int. J. Bifur. Chaos. 1, 0809-0819. 2009.

[5] G. Shambat, B. Ellis, A. Majumdar, J. Petykiewicz, M. Mayer, T. Sarmiento, J. Harris, E. Haller and J. Vuckovic´. Ultrafast direct modulation of a single-mode photonic crystal nanocavity light-emitting diode. Nature communications 10. 1038-1043. 2011.

[6] X. Yang, Y. Ma, E. Mutlugun, Y. Zhao, K. S. Leck, S. T. Tan, H. V. Demir, Q. Zhang, H. Du, and X. Wei Sun. Stable, Efficient, and All-Solution-Processed Quantum Dot Light Emitting Diodes with Double-Sided Metal Oxide Nanoparticle Charge Transport Layers. ACS Appl. Mater. Interfaces 6, 495−499, 2014.

[7] G. Giacomelli, M. Calzavara, F. Arecchi. Instabilities in a semiconductor laser with delayed optoelectronic feedback. Opt Commun 74, 97–101, 1989.

[8] N. Loiko, A. Samson. Possible regimes of generation of a semiconductor laser with a delayed optoelectronic feedback. Opt Commun 93, 66–72, 1992.

[9] E. Lee, H. Pang, J. Park, H. Lee, "Bistability and chaos in an injection locked semiconductor laser. ", Phys Rev A 47, 736–739, 1993.

[10] K. Al-Naimee, F. Marino, M. Ciszak, R. Meucci, and F. T. Arecchi, "Chaotic spiking and incomplete homoclinic scenarios in semiconductor lasers with optoelectronic feedback. ", New J. Phys. 11, 073022, 2009.

[11] M. Bertram and A. S. Mikhailov, "Pattern formation in a surface chemical reaction with global delayed feedback. ", Phys. Rev. E 63, 066102, 2001.

[12] S. Tang, JM. Liu, "Chaotic pulsing and quasi-periodic route to chaos in a semiconductor laser with delayed opto-electronic feedback. ", IEEE J Quantum Electron 37, 329–336, 2001.

[13] Y. Liu, P. Davis, Y. Takiguchi, T. Aida, A. Saito and J. M. Liu, "Digital Communications Using Chaos and Nonlinear Dynamics. ", IEEE J. Quantum Electron. 39, 269, 2003.

[14] A. Uchida, Y. Liu, I. Fischer, P. Davis and T. Aida, "Chaotic antiphase dynamics and synchronization in multimode semiconductor lasers. ", Phys. Rev. A64, 023801, 2001.

[15] T. Heil, I. Fischer, W. Elsasser, J. Mulet and C. R. Mirasso, "Chaos synchronization and spontaneous symmetry breaking in symmetrically delay coupled semiconductor lasers. ", Phys. Rev. Lett. 86, 795, 2001.

[16] D. M. Kane, J. P. Toomey, M. W. Lee and K. A. Shore, "Correlation Dimension Signature of Wideband Chaos synchronization of Semiconductor Lasers. ", Opt. Lett. 31, 20, 2006.

[17] S. Tang and J. M. Liu, "Chaotic pulsing and quasi-periodic route to chaos in a semiconductor laser with delayed optoelectronic. ", Phys. Rev. Lett. 90, 194101, 2003.

[18] S. Tang and J. M. Liu, "Communication using synchronization of optical feedback-induced chaos in semiconductor lasers. ", IEEE J. Quantum Electron. 39, 963, 2003.

[19] F. Marino, M. Ciszak, S. F. Abdalah, K. Al-Naimee,R. Meucci, and F. T. Arecchi, "Mixed-mode oscillations via canard explosions in light-emitting diodes with optoelectronic feedback. ", Phy. Rev. E 84, 047201, 2011.

[20] S. Fan, P. R. Villeneuve, and J. D. Joannopoulos, "Rate-Equation Analysis of Output Efficiency and Modulation Rate of Photonic-Crystal Light-Emitting Diodes. ", IEEE journal of quantum electronics, 36, 10, 2000.

[21] S.F. Abdalah, K. Al-Naimee, F. Marino, M. Ciszak, R. Meucci and F.T. Arecchi, "chaos and mixed mode oscillations in optoelectronic networks. ", IREPHY. 7, 3. 2013.

[22] B. A. Ghalib, S. J. Al-Obaidi, A. H. Al-Khursan, "Quantum dot semiconductor laser with optoelectronic feedback. ", Superlattices and Microstructures, 52, 5, 977-986, 2012.

[23] K. Al Naimee, H. Al Husseini, S.F. Abdalah, A. Al Khursan, A.H. Khedir, R. Meucci, F.T. Arecchi, "Complex dynamics in Quantum Dot Light Emitting Diodes," Eur. Phys. J. D, 69: 257, 1-5, 2015.

[24] F. Lin, J. Liu, "Nonlinear dynamics of a semiconductor laser with delayed negative optoelectronic feedback. ", IEEE J Quantum Electron, 39, 562–568, 2003.

[25] Sadeq Kh. Ajeel • Rajaa Hussein Abd Ali • Salam K. Mousa • Hussein B. Al Husseini, *Theoretical evidence for synchronous and multi-scroll attractors in coupled quantum dot light-emitting diode*, J Opt. The Optical Society of India 2021. https://doi.org/10.1007/s12596-021-00793-w

[26] Rajaa H. Abudali; Sadeq Kh. Ajeel; Salam K. Mousa; Hussein B. Al Husseini, "Phase-Coupled Synchronization with Optoelectronic Feedback" 2022 International Congress on Human-Computer Interaction, Optimization and Robotic Applications (HORA). IEEE. Ankara, Turkey. 10.1109/HORA55278.2022.9799889

[27] Seham A.AlJabri1· Hussein B. Al Husseini," Effect of phase conjugate coupled on routes to chaos in incoherent optical feedback semiconductor quantum dot laser" J Opt, The Optical Society of India 2022. https://doi.org/10.1007/s12596-022-00894-0.

[28] Tareq A. Al Attabi and Hussein B. Al Husseini '"Equilibrium points, linear stability, and bifurcation analysis on the dynamics of a quantum dot light emitting diode system" Journal of Optical Communications. Published online by De Gruyter November 7, 2022. https://doi.org/10.1515/joc-2022-0154